Effects of Spin and Exchange Interaction on the Coulomb-Blockade Peak Statistics in Quantum Dots

Y. Alhassid and T. Rupp

Center for Theoretical Physics, Sloane Physics Laboratory, Yale University, New Haven, Connecticut 06520, USA

(Received 9 December 2002; published 30 July 2003)

We derive a closed expression for the linear conductance through a quantum dot in the Coulomb-blockade regime in the presence of a constant exchange interaction. With this expression we calculate the temperature dependence of the conductance peak-height and peak-spacing statistics in chaotic quantum dots. Using a realistic value of the exchange interaction, we find significantly better agreement with experimental data as compared with the statistics obtained in the absence of exchange.

DOI: 10.1103/PhysRevLett.91.056801 PACS numbers: 73.23.Hk, 05.45.Mt, 73.40.Gk, 73.63.Kv

The conductance through a quantum dot that is weakly coupled to leads displays sharp peaks as an applied gate voltage is varied. Each conductance peak describes the addition of one more electron into the dot. The statistics of both the peak heights and peak spacings in dots whose single-electron dynamics is chaotic have been intensively studied in recent years [1]. In such dots the fluctuations of the single-particle levels and wave functions are described by random-matrix theory (RMT) [2]. Some of the experimental observations, e.g., the peak-height distributions at low temperature [3,4], have been explained at least qualitatively by the constant-interaction (CI) model, in which the interaction is represented in the simple form of an electrostatic charging energy. Other observables, such as the peak-spacing distribution [5], have indicated that residual interactions beyond charging energy should be taken into account [6,7].

Recently, a universal Hamiltonian was derived [8,9] for a dot with a large Thouless conductance $g_T \sim \sqrt{N}$ (N is the number of electrons). An important contribution to this Hamiltonian is a constant exchange interaction. The remaining interaction terms are suppressed at large g_T. Effects of the exchange interaction at finite temperature (and finite-g_T corrections) have explained features of the peak-spacing distribution [10,11], but these studies were limited to low temperatures.

Here we study the effects of the exchange interaction and spin on the finite-temperature statistics of both the peak heights and peak spacings over the full measured temperature range. To this end, we derive a closed formula for the conductance in the presence of a constant exchange interaction, expressing the conductance in terms of quantities that characterize spinless noninteracting electrons. We then calculate the finite-temperature peak-height and peak-spacing statistics and find that they are both sensitive to the exchange interaction. Using an RPA estimate of the exchange interaction for the samples studied in Refs. [5,12], we obtain very good agreement with the observed temperature dependence of the standard deviation of the peak spacing for all measured temperatures. We also explain the discrepancies between the experimental peak-height statistics [12] and the predictions of the CI model for $kT \lesssim 0.6\Delta$ (Δ is the mean spacing between spin-degenerate levels).

The universal Hamiltonian of a quantum dot in the limit $g_T \to \infty$ is given by [8,9]

$$\hat{H} = \sum_{\lambda\sigma} \epsilon_\lambda a^\dagger_{\lambda\sigma} a_{\lambda\sigma} + \frac{e^2}{2C}\hat{n}^2 - J_s \hat{\mathbf{S}}^2, \tag{1}$$

where ϵ_λ are spin-degenerate single-particle levels ($\sigma = \pm 1$ labels the spin). The second term in Eq. (1), where C is the dot's capacitance and $\hat{n}$ is the particle-number operator, is the electrostatic energy of the dot. The third term, in which $\hat{\mathbf{S}}$ is the total-spin operator, is a constant exchange interaction with strength J_s. The occupation-number operator $\hat{n}_\lambda = \hat{n}_{\lambda+} + \hat{n}_{\lambda-}$ of any single-particle orbital λ commutes with the total spin, $[\hat{n}_\lambda, \hat{\mathbf{S}}] = 0$, and the Hamiltonian $\hat{H}$ is invariant under spin rotations. Thus the eigenstates of $\hat{H}$ are characterized by their particle number N, the orbital occupation numbers $\mathbf{n} = \{n_\lambda\}$ ($n_\lambda = 0$, 1, or 2), the total spin S, and its projection $S_z = M$. We label the eigenstates as $|N\mathbf{n}\gamma SM\rangle$ where γ distinguishes between states with the same total spin S and particle configuration $\mathbf{n}$. The eigenenergies are given by $\varepsilon^{(N)}_{\mathbf{n}S} = \sum_\lambda \epsilon_\lambda n_\lambda + e^2N^2/2C - J_s S(S+1)$.

When a typical tunneling width is small compared with kT and Δ, the conductance can be calculated using a rate-equations approach. Reference [13] describes such an approach in the presence of interactions and spin. In particular, an explicit solution exists in the special case when n_λ are good quantum numbers. Expressing the conductance G in a rescaled form $g = G/(e^2\bar{\Gamma}/8\hbar kT)$ ($\bar{\Gamma}$ is an average width of a level), we have, in the vicinity of the $N+1$st Coulomb-blockade peak [10,13]

$$g = 4\sum_{\substack{\lambda\mathbf{n}\gamma S\\ \mathbf{n}'\gamma' S'}} \tilde{P}^{(N)}_{\mathbf{n}S} f(\varepsilon^\lambda_{S'S}) |([N+1]\mathbf{n}'\gamma' S' \| a^\dagger_\lambda \| N\mathbf{n}\gamma S)|^2 g_\lambda. \tag{2}$$

Here $g_\lambda = 2\bar{\Gamma}^{-1}\Gamma^{\rm l}_\lambda \Gamma^{\rm r}_\lambda/(\Gamma^{\rm l}_\lambda + \Gamma^{\rm r}_\lambda)$ are the single-particle level conductances, where $\Gamma^{\rm l,r}_\lambda$ are the partial widths of an electron in orbital λ to decay to the left or right lead. The equilibrium probability of the dot to be in the state $|N\mathbf{n}\gamma SM\rangle$ is $\tilde{P}^{(N)}_{\mathbf{n}S} = e^{-\beta[\varepsilon^{(N)}_{\mathbf{n}S} - \tilde{\epsilon}_F N]}/Z$, where the partition function Z is a Boltzmann-weighted sum over all possible N- and $(N+1)$-body states, and $\tilde{\epsilon}_F = e\zeta V_g + \epsilon_F$ is an effective Fermi energy (ϵ_F is the Fermi energy in the leads, V_g is the gate voltage, and $\zeta = C_g/C$ with C_g the dot-gate capacitance). The Fermi-Dirac function $f(x) = (1 + e^{\beta x})^{-1}$ is evaluated at an electron energy $\varepsilon^{\lambda}_{S'S} = \varepsilon^{(N+1)}_{\mathbf{n}'S'} - \varepsilon^{(N)}_{\mathbf{n}S} - \tilde{\epsilon}_F$ that conserves energy at the transition between states $|N\mathbf{n}\gamma SM\rangle$ and $|(N+1)\mathbf{n}'\gamma' S'M'\rangle$. The reduced matrix element $([N+1]\mathbf{n}'\gamma' S'\|a^\dagger_\lambda\|N\mathbf{n}\gamma S)$ enforces the selection rule $S' = |S \pm 1/2|$.

Equation (2) requires a summation over the dot's many-body eigenstates, whose number increases combinatorially with the number of single-particle levels. The equation thus becomes impractical at higher temperatures. Here we derive a novel formula for the conductance that is expressed solely in terms of a sum over single-particle levels (and the allowed spin values) and greatly facilitates the calculation of the conductance at higher temperatures. We begin by rewriting Eq. (2) in the form

$$g = \sum_\lambda [w^{(0)}_\lambda + w^{(1)}_\lambda] g_\lambda, \tag{3}$$

where the contributions with $n_\lambda = 0$ and $n_\lambda = 1$ are collected in $w^{(0)}_\lambda$ and $w^{(1)}_\lambda$, respectively. For the cases with $n_\lambda = 0$, the final $(N+1)$-particle state is given by $|(N+1)\mathbf{n}'\gamma' S'M'\rangle = \sum_{M\sigma} (SM\frac{1}{2}\sigma|S'M') a^\dagger_{\lambda\sigma}|N\mathbf{n}\gamma SM\rangle$, where $(SM\frac{1}{2}\sigma|S'M')$ is a Clebsch-Gordan coefficient. When $n_\lambda = 1$ (and hence $n'_\lambda = 2$), the N-particle state can be similarly related to the $(N+1)$-particle state by changing to a hole representation. This leads to

$$([N+1]\mathbf{n}'\gamma' S'\|a^\dagger_\lambda\|N\mathbf{n}\gamma S) = (-)^{S-S'-1/2}\begin{cases}\sqrt{2S'+1} & \text{if } n_\lambda = 0,\\ \sqrt{2S+1} & \text{if } n'_\lambda = 2.\end{cases} \tag{4}$$

Using the relation $\tilde{P}^{(N)}_{\mathbf{n}S} f(\epsilon^\lambda_{S'S}) = \tilde{P}^{(N+1)}_{\mathbf{n}'S'}[1 - f(\epsilon^\lambda_{S'S})]$, we obtain

$$w^{(0)}_\lambda = 4\sum_S b_{\lambda,N,S} P_{N,S} \sum_{S'=S\pm 1/2} (2S'+1) f(\epsilon^\lambda_{S'S}), \tag{5a}$$

$$w^{(1)}_\lambda = 4\sum_{S'} c_{\lambda,N+1,S'} P_{N+1,S'} \sum_{S=S'\pm 1/2} (2S+1)[1 - f(\epsilon^\lambda_{S'S})], \tag{5b}$$

where the quantities $b_{\lambda,N,S} = \frac{1}{2}\langle(\hat{n}_\lambda - 1)(\hat{n}_\lambda - 2)\rangle_{N,S}$ and $c_{\lambda,N,S} = \frac{1}{2}\langle\hat{n}_\lambda(\hat{n}_\lambda - 1)\rangle_{N,S}$ ensure that the sum is only over contributions with $n_\lambda = 0$ or 1, respectively. They are defined as thermal expectation values at constant particle number N and spin S, i.e., $\langle\hat{X}\rangle_{N,S} = \mathrm{Tr}_{N,S}[\hat{X}e^{-\beta\hat{H}}]/\mathrm{Tr}_{N,S}[e^{-\beta\hat{H}}]$. The quantity $P_{N,S}$ is the probability to find the dot with N electrons and spin S,

$$P_{N,S} = e^{-\beta[F_{N,S} + U_{N,S}]}/Z, \tag{6}$$

where $F_{N,S} = -\beta^{-1}\ln\mathrm{Tr}_{N,S} e^{-\beta\sum_{\lambda\sigma}\epsilon_\lambda a^\dagger_{\lambda\sigma}a_{\lambda\sigma}}$ is the free energy of N noninteracting electrons with total spin S and $U_{N,S} = e^2N^2/2C - J_s S(S+1) - \tilde{\epsilon}_F N$.

The spin-projected trace of a scalar observable can be calculated from traces at fixed spin projection M using $\mathrm{Tr}_{N,S}\hat{X} = \mathrm{Tr}_{N,M=S}\hat{X} - Tr_{N,M=S+1}\hat{X}$. For spin-1/2 particles, the projection on fixed particle number N and spin projection M is equivalent to projecting on a fixed number of spin-up and spin-down particles $n_\pm = N/2 \pm M$. Therefore, $\mathrm{Tr}_{N,S}\hat{X} = \mathrm{tr}_{N/2+S,N/2-S}\hat{X} - \mathrm{tr}_{N/2+S+1,N/2-(S+1)}\hat{X}$, where the traces "tr" on the right-hand side are evaluated at fixed n_+ and n_-. Using $\hat{X} = e^{-\beta\sum_{\lambda\sigma}\epsilon_\lambda a^\dagger_{\lambda\sigma}a_{\lambda\sigma}}$, we find that the free energy in Eq. (6) is given by

$$e^{-\beta F_{N,S}} = e^{-\beta[\tilde{F}_{N/2+S} + \tilde{F}_{N/2-S}]} - e^{-\beta[\tilde{F}_{N/2+S+1} + \tilde{F}_{N/2-(S+1)}]}. \tag{7}$$

The free energy $\tilde{F}_q$ in Eq. (7) is defined for q spinless fermions $e^{-\beta\tilde{F}_q} = \mathrm{tr}_q e^{-\beta\sum_\lambda \epsilon_\lambda c^\dagger_\lambda c_\lambda}$, where $c^\dagger_\lambda$ create spinless fermions in nondegenerate levels ϵ_λ. The quantity $c_{\lambda,N,S}$ from Eq. (5b) can now be expressed as

$$c_{\lambda,N,S} = \frac{\langle\tilde{n}_\lambda\rangle_{N/2+S}\langle\tilde{n}_\lambda\rangle_{N/2-S}e^{-\beta[\tilde{F}_{N/2+S} + \tilde{F}_{N/2-S}]} - \langle\tilde{n}_\lambda\rangle_{N/2+S+1}\langle\tilde{n}_\lambda\rangle_{N/2-(S+1)}e^{-\beta[\tilde{F}_{N/2+S+1} + \tilde{F}_{N/2-(S+1)}]}}{e^{-\beta[\tilde{F}_{N/2+S} + \tilde{F}_{N/2-S}]} - e^{-\beta[\tilde{F}_{N/2+S+1} + \tilde{F}_{N/2-(S+1)}]}}, \tag{8}$$

where $\tilde{n}_\lambda$ is the particle-number operator of a nondegenerate orbital λ. The function $b_{\lambda,N,S}$ from Eq. (5a) is expressed by replacing $\tilde{n}_\lambda$ by $(1 - \tilde{n}_\lambda)$ in Eq. (8). The complete expression for the conductance is then obtained from Eqs. (3) and (5)–(8) and the relation indicated in the previous sentence. Thus the dot's conductance in model (1) is determined in terms of the free energy $\tilde{F}_q$ and occupation numbers $\langle\tilde{n}_\lambda\rangle_q$ of q noninteracting spinless fermions, quantities that are familiar from the CI model [14] and can be expressed in closed form using particle-number projection [see Eqs. (140) in Ref. [1]].

In chaotic dots, the single-particle Hamiltonian in (1) is described by RMT [2]. We have studied the statistics of peak heights and spacings for both the orthogonal and unitary symmetries using a rather large space of 50 single-particle orbitals λ. We verified that our results are not affected by the finite size of the system up to temperatures of $kT \sim 3\Delta$. The results shown below (except in Fig. 4) are for the unitary statistics (i.e., in the presence of a nonzero perpendicular magnetic field).

Theoretical calculations of the width $\sigma(\Delta_2)$ of the peak-spacing distribution, based on a spinless CI model [15], describe qualitatively the observed decrease of this quantity with increasing temperature [5]. However, when spin is included and in the absence of exchange, the calculated values of $\sigma(\Delta_2)$ (long-dashed line in Fig. 1) show a large discrepancy with the experimental values (symbols). Figure 1 also shows $\sigma(\Delta_2)$ for nonzero values of J_s. For a gas constant of $r_s \sim 1.2$ (which corresponds to the samples used in the experiments), the RPA estimate is $J_s \approx 0.3\Delta$ [16], and we find for this value a very good agreement with the measurements. The results for $J_s = 0.5\Delta$ (a limiting RPA value for large r_s) underestimate the experimental widths. We remark that at temperatures $kT \lesssim 0.4\Delta$, model (1) does not describe well the shape of the peak-spacing distribution, and it is necessary to include the fluctuating part of the interaction to explain the absence of bimodality [7,10,11]. At higher temperatures, the bimodality is absent already in model (1) and the residual interaction has a negligible effect on the width.

Next, we discuss the peak-height statistics [17]. An important measured quantity is the ratio between the standard deviation $\sigma(g_{\max})$ and the average $\bar{g}_{\max}$ of the peak heights $g_{\max}$ [12]. The experimental data for this ratio (symbols in Fig. 2) are suppressed in comparison with the results of model (1) without an exchange term (long-dashed line in the left panel of Fig. 2). Spin-orbit interaction has been proposed as a mechanism for this suppression [18]. It was necessary to assume a spin-orbit coupling that is sufficiently strong to decorrelate the spin-up and spin-down levels. However, spin-orbit effects are likely to be suppressed in small dots [19]. To determine whether an exchange interaction can explain the observed suppression of $\sigma(g_{\max})/\bar{g}_{\max}$, we calculated this ratio versus kT for different strengths of J_s (see Fig. 2). In the elastic limit (left panel), a realistic exchange interaction of $J_s = 0.3\Delta$ (solid line) leads to closer agreement with the data. The remaining small discrepancy at $kT \lesssim 0.6\Delta$ can probably be accounted for by adding a realistic weak spin-orbit interaction. The discrepancy at higher temperatures, where inelastic scattering may play a role, remains to be explained. The suppression of $\sigma(g_{\max})/\bar{g}_{\max}$ due to inelastic scattering was shown to be small for $J_s = 0$ [20]. In the right panel of Fig. 2 we show results for the rapid-thermalization limit of strong inelastic scattering in the presence of an exchange interaction. These calculations do not describe the high-temperature data, and it would be interesting to determine the effect of an additional weak spin-orbit term.

For $kT \ll \Delta$ and $J_s = 0$, the peak-height distribution $P(g_{\max})$ is known analytically [3] and is shown for the unitary symmetry in the left panel of Fig. 3 (solid line). Also shown (histogram) is the peak-height distribution calculated at $kT = 0.01\Delta$ and $J_s = 0.5\Delta$. No significant effect due to exchange is observed except for a small enhancement of the probability at small peak heights.

At finite temperature, the exchange interaction has a stronger effect on the peak-height distribution. The right panel of Fig. 3 compares the histogram (shaded) of the experimental data for $P(g_{\max}/\bar{g}_{\max})$ at $kT = 0.1\Delta$ with the calculated histograms for the cases of no exchange ($J_s = 0$) and $J_s = 0.3\Delta$. This latter realistic value of the exchange interaction explains the observed suppression of the probability at small peak heights.

The weak-localization effect in the average peak height has recently attracted attention both in experiment

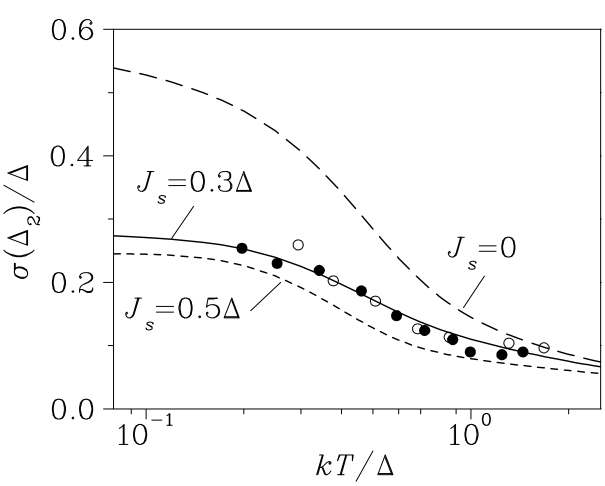

FIG. 1. The width $\sigma(\Delta_2)$ of the peak-spacing distribution (unitary symmetry) for different values of the exchange interaction J_s. The symbols are the experimental data of Ref. [5].

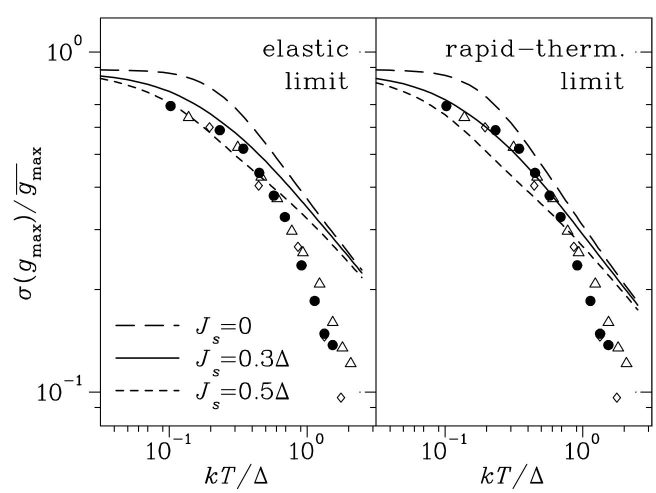

FIG. 2. The ratio $\sigma(g_{\max})/\bar{g}_{\max}$ between the standard deviation and the average value of the peak height versus temperature kT for the unitary statistics. The left (right) panel shows the elastic (rapid-thermalization) limit for $J_s = 0$ (long-dashed), 0.3Δ (solid), and 0.5Δ (short-dashed). The symbols are the experimental data of Ref. [12].

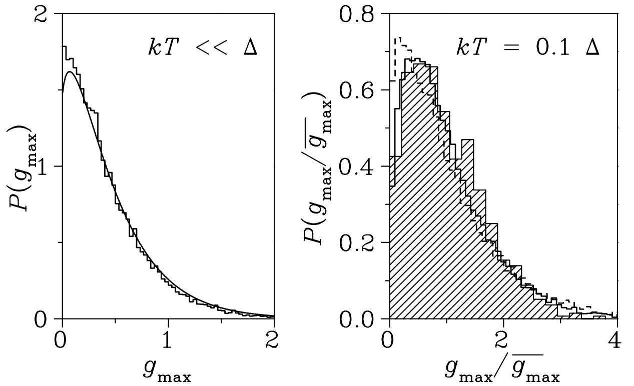

FIG. 3. Peak-height distributions (unitary symmetry). Left panel: The distribution $P(g_{max})$ at $kT \ll \Delta$ and $J_s = 0$ (smooth line) is compared with the corresponding distribution at $kT = 0.01\Delta$ and $J_s = 0.5\Delta$ (histogram). Right panel: Experimental data from Ref. [12] (shaded histogram) at $kT = 0.1\Delta$ are compared with the calculated distributions at $J_s = 0$ (dashed histogram) and $J_s = 0.3\Delta$ (solid histogram).

and theory [20–23]. Its suppression at higher temperatures was suggested as a signature of inelastic scattering [22]. The effect is quantified by the parameter $\alpha = 1 - (\bar{g}_{\max}^{\rm GOE}/\bar{g}_{\max}^{\rm GUE})$. In the rapid-thermalization limit, α decreases rapidly with increasing temperature from its value of 0.25 at $kT \ll \Delta$. In contrast, if inelastic scattering is negligible, α was expected to be temperature independent. However, calculations for $J_s = 0$ showed a slight suppression of the elastic α around $kT \sim 0.25\Delta$ [20,23]. This was understood by the fact that close-lying levels and hence higher conductances are more likely for the orthogonal symmetry. The effect of the exchange interaction on α is shown in Fig. 4. We find that the dip

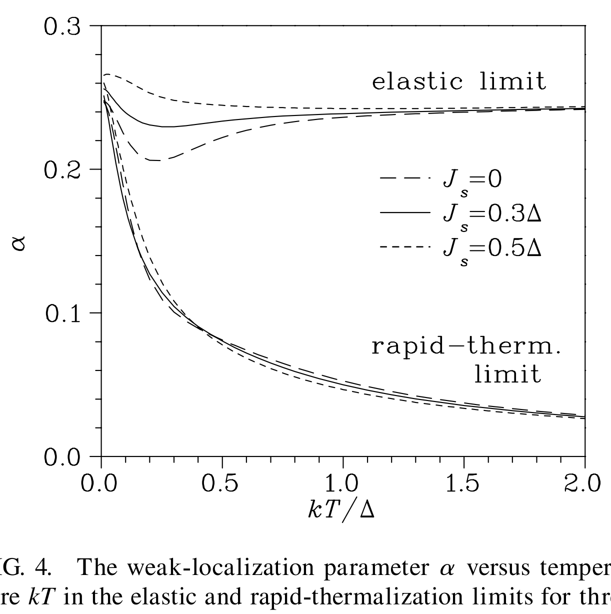

FIG. 4. The weak-localization parameter α versus temperature kT in the elastic and rapid-thermalization limits for three different values of the exchange-interaction strength J_s.

in α around $kT \sim 0.25\Delta$ is flattened out and in the small-temperature limit α becomes larger than 0.25 [10]. However, the experimental errors of Ref. [21] are too large to observe this effect. In the rapid-thermalization limit, α is rather insensitive to J_s (see Fig. 4).

In conclusion, we have derived a closed expression for the conductance in the presence of spin and exchange interaction. Using this formula we studied the dependence of both the peak-height and peak-spacing statistics on the exchange interaction and found a significantly better quantitative agreement with experiment as compared with calculations in the absence of exchange.

This work was supported in part by the U.S. DOE Grant No. DE-FG-0291-ER-40608. We thank C. M. Marcus for helpful discussions.

[1] Y. Alhassid, Rev. Mod. Phys. **72**, 895 (2000).
[2] T. Guhr, A. Müller-Groeling, and H. A. Weidenmüller, Phys. Rep. **299**, 189 (1998).
[3] R. A. Jalabert, A. D. Stone, and Y. Alhassid, Phys. Rev. Lett. **68**, 3468 (1992).
[4] A. M. Chang *et al.*, Phys. Rev. Lett. **76**, 1695 (1996); J. A. Folk *et al.*, Phys. Rev. Lett. **76**, 1699 (1996).
[5] S. R. Patel *et al.*, Phys. Rev. Lett. **80**, 4522 (1998).
[6] R. Berkovits, Phys. Rev. Lett. **81**, 2128 (1998).
[7] A. D. Mirlin, Phys. Rep. **326**, 259 (2000).
[8] I. L. Kurland, I. L. Aleiner, and B. L. Altshuler, Phys. Rev. B **62**, 14 886 (2000).
[9] I. L. Aleiner, P.W. Brouwer, and L. I. Glazman, Phys. Rep. **358**, 309 (2002).
[10] G. Usaj and H. U. Baranger, Phys. Rev. B **64**, 201319R (2001); **66**, 155333 (2002).
[11] Y. Alhassid and S. Malhotra, Phys. Rev. B **66**, 245313 (2002).
[12] S. R. Patel *et al.*, Phys. Rev. Lett. **81**, 5900 (1998).
[13] Y. Alhassid, T. Rupp, A. Kaminski, and L. I. Glazman, cond-mat/0212072.
[14] C.W. J. Beenakker, Phys. Rev. B **44**, 1646 (1991).
[15] Y. Alhassid and S. Malhotra, Phys. Rev. B **60**, R16 315 (1999).
[16] Y. Oreg *et al.*, in *Nano-Physics and Bio-Electronics: a New Odyssey*, edited by T. Chakraborty, F. Peeters, and U. Sivan (Elsevier, New York, 2002).
[17] After completing this work, we learned of G. Usaj and H. U. Baranger, Phys. Rev. B **67**, 121308R (2003), which studies the peak-height statistics for $J_s \neq 0$ and $kT \leq \Delta$.
[18] K. Held, E. Eisenberg, and B. L. Altshuler, Phys. Rev. Lett. **90**, 106802 (2003).
[19] D. M. Zumbühl *et al.*, Phys. Rev. Lett. **89**, 276803 (2002).
[20] T. Rupp, Y. Alhassid, and S. Malhotra, Phys. Rev. B **65**, 193304 (2002).
[21] J. A. Folk, C. M. Marcus, and J. S. Harris, Jr., Phys. Rev. Lett. **87**, 206802 (2001).
[22] C.W. J. Beenakker, H. Schomerus, and P. G. Silvestrov, Phys. Rev. B **64**, 033307 (2001).
[23] E. Eisenberg, K. Held, and B. L. Altshuler, Phys. Rev. Lett. **88**, 136801 (2002).